Interface states, negative differential resistance, and rectification in molecular junctions with transition-metal contacts

Hugh Dalgleish and George Kirczenow
Department of Physics, Simon Fraser University, Burnaby, British Columbia, Canada V5A 1S6
(Received 9 February 2006; revised manuscript received 12 April 2006; published 26 June 2006)

We present a theory of nonlinear transport phenomena in molecular junctions where single thiolated organic molecules bridge transition metal nanocontacts whose densities of states have strong *d* orbital components near the Fermi level. At moderate bias, we find electron transmission between the contacts to be mediated by interface states within the molecular highest-occupied-molecular-orbital–lowest-unoccupied-molecular-orbital gap that arise from hybridization between the thiol-terminated ends of the molecules and the *d* orbitals of the transition metals. Because these interface states are localized mainly within the metal electrodes, we find their energies to accurately track the electrochemical potentials of the contacts when a variable bias is applied across the junction. We predict resonant enhancement and reduction of the interface state transmission as the applied bias is varied, resulting in negative differential resistance (NDR) in molecular junctions with Pd nanocontacts. We show that these nonlinear phenomena can be tailored by suitably choosing the nanocontact materials: If a Rh electrode is substituted for one Pd contact, we predict enhancement of these NDR effects. The same mechanism is also predicted to give rise to rectification in Pd/molecule/Au junctions. The dependences of the interface state resonances on the orientation of the metal interface, the adsorption site of the molecule, and the separation between the thiolated ends of the molecule and the metal contacts are also discussed.

DOI: 10.1103/PhysRevB.73.245431 PACS number(s): 73.63.−b, 85.65.+h, 73.20.−r, 73.40.Ei

I. INTRODUCTION

Metal/molecule/metal junctions are currently the focus of intense research, owing to both the promise of future electronic device applications and the challenges they present to fundamental science. A particular challenge stems from the realization that the properties of molecular junctions are strongly influenced by the *combined* characteristics of the molecule and metal contacts.[1–22] As a result, structural and chemical characteristics of the metal-molecule interface are expected to significantly affect the transport properties of molecular junctions. Many theoretical studies have elucidated the nature of such effects in gold/molecule/gold junctions for which the influence of the specifics of the molecules themselves and of the atomic geometry of the Au interface on transport has been investigated in great detail.[2,4,5,7,8,11,13,16,20,22–26] However, there has also been interest in molecular junctions with other noble metals[3,6,27] and with transition metal contacts such as Ni,[28–31] Fe,[32] Pt,[6,19,33–36] and Pd.[6,36,37]

For thiolated molecules bridging Au electrodes, very weakly transmitting hybridized molecular-contact states have been predicted within the molecular highest-occupied-molecular-orbital–(HOMO–) lowest-unoccupied-molecular-orbital (LUMO) gap.[13,26] These metal-induced gap states (MIGS) or interface states (as their wave functions are spatially localized at the metal-molecule interface) form as a result of hybridization between molecular thiol groups and surface states of the metal contacts. In Au/molecule/Au molecular junctions, these interface states have been shown to play only a *minimal* role in transport.[13,26] In Ni and Fe molecular junctions, however, metal-molecule interface states have been predicted to *dominate* the transport at low bias leading to unusual transport phenomena such as large magnetoresistance[28–31] and inversion of the magnetoresistance under bias.[32] Important differences between the Au and magnetic metal-molecule junctions that lead to the crucial role played by interface states in systems of the latter type have been attributed to the nontrivial *d*-electron character of the magnetic electrodes near the Fermi energy.[31,32] Similarly, interface states that form near the Fermi energy due to hybridization between thiolated molecules and *d*-electron states of Pt,[6,19,33,34] Pd,[6] and other transition metal[6] electrodes have been predicted to produce larger low bias conductances than for systems based on Au where *d* orbitals play a relatively minor role. However, these theoretical studies of thiolated organic molecules on Pt and Pd electrodes have not considered explicitly the effects of bias on the interface state transmission, which can give rise to strongly nonlinear transport phenomena. Also, the systematic evolution of interface state transmission as the molecule-metal bonding geometry is varied has not been investigated.

In this article we investigate the transport properties that emerge when simple organic molecules bridge nonmagnetic electrodes that have more complex electronic structure than Au leads. As a prototype system, we study a single four-alkane-dithiolate molecule (butyl-dithiolate with four carbon atoms, hereafter denoted AT4) bridging Pd contacts, however, our qualitative findings are applicable to a wide range of molecular junctions consisting of different thiolated molecules bridging a variety of metal contacts with *d*-electronic states near the Fermi energy.[38] We then investigate the effect that replacing one of the Pd electrodes with either a Rh or Au contact has on the calculated transmission.

We find the nontrivial *d*-electron character of the Pd (or Rh) electrodes to result in interesting transport properties (different from those of Au molecular junctions) that are due to interface states between the molecular sulfur atoms and the metal contacts that form within the molecular HOMO-LUMO gap. These interface states dominate the transmission

through the junction at moderate bias. We show that under bias the energies of these interface states lock to the shifting electrochemical potentials of the contacts.[39] We predict that for some values of the bias they should resonantly enhance the transmission, giving rise to nonlinear transport phenomena including negative differential resistance (NDR) and rectification. Thus we introduce a mechanism for both NDR and rectification in molecular junctions, that differs from previously proposed mechanisms[9–11,17,21,23,40–63] in that here resonant interface state transmission is the source of these phenomena. Furthermore, our results indicate that these transport phenomena are strongly dependent on the atomic parameters of the molecular junctions, which in principle will depend on how samples are fabricated.[22] Thus our results offer avenues for control of the properties of nonlinear molecular electronic devices.

This article is organized as follows. In Sec. II we describe our model of the geometries and electronic structures of the molecular junctions, and also briefly summarize the formalism used in our transport calculations. In Sec. III our formalism is applied to Pd/AT4/Pd molecular junctions at zero bias where we discuss in detail the nature of the interface states that dominate the transmission probability at moderate bias. We then proceed to study the evolution of the interface states as the Pd electrodes are brought into increasingly close contact with the molecule. Next we study the dependence of the shape, strength and energy location of the interface state transmission resonances on the interfacial binding site and Pd crystal surface orientation. We also examine the effect that increasing the length of the molecular carbon backbone has on the interface state transmission and extract a decay parameter β from our calculations. Our value for β is compared to previous theoretical and experimental results for related alkane-thiol systems. Once the nature of these interface states have been elucidated, we consider explicitly the effect of bias on the transmission. The interface resonances are shown to shift rigidly with applied bias leading to enhancements in the transmission as a function of applied bias, and an intuitive two-level model is presented to explain these resonant enhancements. Finally we show that these transmission enhancements under bias give rise to nonlinear transport phenomena including negative differential resistance and rectification, and that those phenomena may be tailored by substituting either a Rh or Au electrode for one of the Pd electrodes. Our conclusions are summarized in Sec. IV.

II. THEORY

In our calculations the system is partitioned into semi-infinite ideal source and drain leads and an extended molecular junction consisting of the molecule and clusters of nearby metal (Pd, Rh, or Au) atoms. The metal atoms are arranged in bulk fcc geometries and the metal-thiol bonding geometries are estimated with *ab initio* relaxations.[64]

The electronic structure of the metal (Pd, Rh, and Au) clusters is described by a tight-binding Hamiltonian and nonorthogonal s,p,d basis. The tight-binding parameters are based on fits to *ab initio* nonmagnetic band structures of the metal crystals;[65–67] in the case of Pd, tight-binding[68,69] and extended-Hückel[70] descriptions have previously been employed to study structure and electronic characteristics of Pd nanoclusters with results comparable to density functional descriptions. When used to describe Fe nanoclusters,[32,71] this model yielded magnetic moments for surface and interior atoms in very close agreement with *ab initio* calculations.[72] Parameters taken from Ref. 65 have been successfully employed to study transport in magnetic nanocontacts,[71,73] and ferromagnetic Ni (Ref. 28) and Fe (Ref. 32) molecular junctions in all of which metal d-states play important roles. Furthermore, tight-binding parameters taken from Ref. 65 have been used to model Pt nanocontacts (the electronic structure of Pt is similar to Pd), and the resulting transport properties have been shown to agree with a density functional theory description of the Pt contacts.[74] Thus it seems reasonable to extend this parameterization to model nanoscale tips of bulk metal leads as we do here.

The molecular electronic parameters as well as the electronic parameters describing the molecular coupling to the electrodes are described by a tight-binding formalism based on extended-Hückel (EH) theory.[75] This approach has been used successfully to explain the experimental current-voltage characteristics of molecular nanowires connecting Au electrodes.[10,23,24] The EH parameters are based on atomic ionization energies while the electronic parameters from Ref. 65 describing the Pd, Rh, or Au metal clusters are defined up to an arbitrary additive constant. We adjust this constant to align the Fermi energy of the contacts relative to the highest occupied molecular orbital (HOMO) of the AT4 molecule, according to the difference between the work function of the metal and the HOMO energy of the isolated molecule obtained from density functional theory,[64] a method that has been used successfully to align the Fermi energy of gold with the HOMO of benzene-dithiolate (BDT).[25]

Our transport calculations are based on Landauer theory[76] and Lippmann-Schwinger and Green's function techniques. Landauer theory relates the current to the multichannel probability T for an electron to scatter from the source electrode to the drain via the junction, according to

$$I(V) = \frac{2e}{h} \int dE\, T(E,V)[f(E,\mu_S) - f(E,\mu_D)], \qquad (1)$$

where E is the energy of the electron, $f(E,\mu)$ is the equilibrium Fermi distribution, and $\mu_{S,D}=E_F \pm eV/2$ are the electrochemical potentials of the source (S) and drain (D) electrodes in terms of the common Fermi energy E_F. Our convention of current flow is that the source electrode is the source for electron flux. A detailed discussion of our theoretical formalism has been presented elsewhere.[71]

III. RESULTS

The Pd/AT4/Pd molecular junction is displayed in the left inset of Fig. 1(a). Each Pd cluster of the extended molecule is built from 5×5, 4×4, 3×3, 2×2 (100)-oriented layers (54 atoms total) of atoms in the bulk geometry of fcc Pd. The sulfur atoms are estimated to sit 1.74 Å above the Pd fcc hollow site.[64]

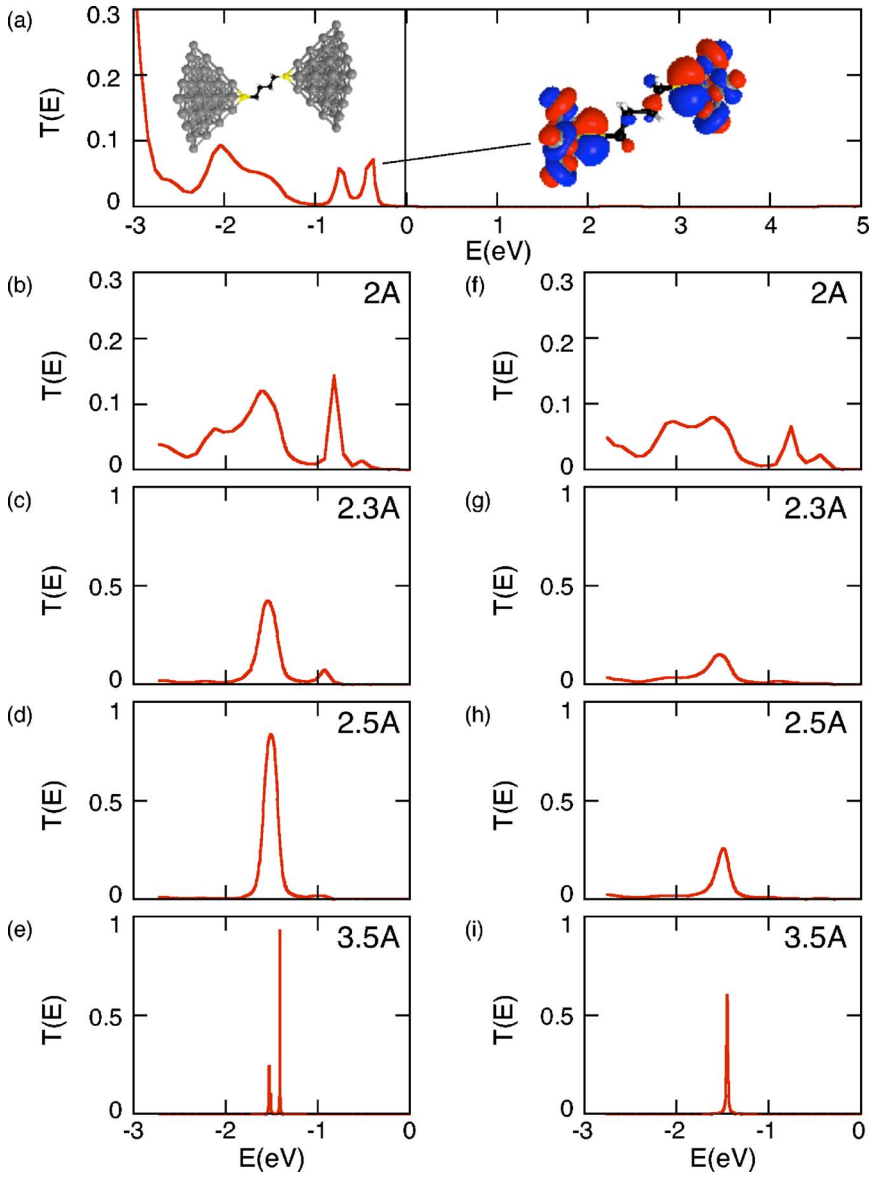

FIG. 1. (Color online) Transmission probabilities at zero bias $T(E,0)$ for increasing thiol-Pd contact separation for the Pd-AT4 molecular junction shown in the inset on the left of (a). (a) Transmission probability vs. energy for equilibrium thiol-Pd separation of 1.74 Å. Fermi energy=0 eV. The inset on the right displays a molecular orbital picture of an interface state with energy in the range of the transmission peak closest to the Fermi energy. (b) Transmission probability with the Pd-S separation increased to 2 Å for both contacts symmetrically. (c) 2.3 Å Pd-S separation. (d) 2.5 Å. (e) 3.5 Å. (f)–(i) Corresponding transmission probabilities in a sequence of STM-like geometries with one Pd-S distance fixed at the equilibrium value and the other varied as in (b)–(e), respectively.

The calculated transmission probability at zero bias for the Pd/AT4/Pd molecular junction is shown in Fig. 1(a). The molecular HOMO gives rise to the broad transmission 1.5–2 eV below the Fermi energy E_F=0 eV; the lowest unoccupied molecular orbital lies outside of the plotted energy range due to the large molecular HOMO-LUMO gap (AT4 is an insulator). More important, however, as they influence the current at lower bias, are resonant states within the HOMO-LUMO gap arising from strong hybridization between the molecular sulfur and Pd *d*-electron surface states. In Fig. 1(a) these states give rise to the relatively sharp transmission features [the double-peaked feature] between the Fermi energy and the HOMO resonances mentioned above. The inset on the right in Fig. 1(a) shows a representative molecular orbital for an interface state with energy in the range of the transmission peak closest to the Fermi energy; interface states responsible for each peak have similar molecular orbital character. The electronic wave function is spatially localized on the sulfur-metal region (the metal-molecule interface) therefore these molecular orbitals are termed "interface states;" not much of the wave function lies on the carbon backbone. Interface states allow electrons to transmit efficiently between the metal and molecule and so give rise to moderately strong transmission dominating the current in the experimentally accessible moderate bias regime, as will be discussed below. As they result from hybridization of the

molecular HOMO, the interface state molecular orbitals on the atoms of the molecule have similar character to that of the HOMO for isolated AT4.

An important difference between the interface state and the HOMO resonances in Fig. 1(a) is that the former appear well within the molecular HOMO-LUMO gap very near the Fermi energy. Another difference is that the interface resonances are due primarily to hybridization of the molecular HOMO with metal *d* orbitals, whereas the HOMO resonance arises primarily from hybridization between the molecular HOMO and metal *s* and *p* orbitals; the interface state resonances completely disappear if the coupling between the metal *d* orbitals and the molecule is switched off. The HOMO resonance does not. The energies of the interface state resonances are comparable to those of Pd *d*-electron orbitals as determined from maxima in the bulk[65] and surface[77] densities of states for Pd.[78]

The sharpness of the interface state transmission features near the Fermi energy relative to the resonances associated with the HOMO reflects the fact that Pd *d*-electron bands are energetically localized. Because transmission through the HOMO is dominated by Pd *s* and *p* electrons which are described by broader energy bands, the molecular HOMO broadens severely [Fig. 1(a)].

These interface state transmission features can be contrasted to Au-BDT systems (Refs. 13 and 24, for example), and to our results for Au-AT4,[79] where the *d*-electron states for Au are below the molecular HOMO in energy and so are largely out of range at low bias, and therefore interface state formation is negligible. We find that in molecular-transition metal systems, such as BDT or AT4 bridging Pd, Pt, Rh, Cr, Mo, Ni, or Fe, where the electron *d* states are close in energy to the Fermi energy, interface states are the dominant feature at low bias. In particular, we find in general that once the interface states have been formed (the molecule-lead separation is at its equilibrium value so that the molecule-lead coupling is strong) the interface state resonances appear close in energy to the maxima in the transition metals' densities of states (both bulk and surface DOS are relevant[80]), which are dominated by *d*-electronic states.

The interface states are located primarily within the metal contacts. Because of this, as will be shown in Sec. III D, the energies of the interface states under bias lock to the shifting electrochemical potentials of the contacts, making their relative energy levels strongly dependent on the bias, leading to resonant enhancements in the transmission (and current through the molecule) for some ranges of bias.

A. Evolution as molecule is contacted

More insight into the interface states and their formation can be gained by studying their evolution as the molecule comes into contact with the leads. To that end, we have studied the transmission through the Pd/AT4/Pd system as a function of increasing separation between the thiols and the Pd contacts. Figure 1(b)–1(e) shows the transmission at zero bias as a function of increasing thiol-Pd separation, where we maintain symmetry of the system by simultaneously varying the Pd-S separations on *both* ends of the molecule. For comparison, in Figs 1(f)–1(i) we show transmission results for a sequence of geometries that should be more readily accessible experimentally; here the thiol-Pd distance is fixed at its equilibrium value on one side of the molecule (the molecule is bonded to that contact), while the distance between the other contact (which may represent an STM tip) and the molecule is allowed to vary. Similar results are predicted in both cases, but the differences arising from increasing the separation are more prominent in the symmetric case.

As the thiol-contact separations are increased from the predicted 1.74 Å equilibrium value to 2 Å, the result for which is shown in Fig. 1(b), the transmission near the Fermi energy remains dominated by interface states. Hybridization of the HOMO occurs for a slightly smaller energy range of Pd electron states and as a result the interface state resonances are located slightly further from the Fermi energy (closer to the molecular HOMO). The interface state resonance becomes larger in magnitude, while the structure of the HOMO resonance also changes. As discussed below, such effects arise not only from changes in the Pd-S coupling, but as a result of changing properties of the whole system and therefore are difficult to quantify *a priori*. As the separation is increased to 2.3 Å, as in Fig. 1(c), the transmission becomes more energetically localized near the HOMO resonance where it grows in magnitude [note the change in the *y* axis scale in Fig. 1(c)] while the interface state resonance is diminished. Also the interface state resonance shifts further towards the broadened HOMO, as hybridization occurs with an even smaller range of Pd electron states. This trend continues as the separation is increased to 2.5 Å [Fig. 1(d)], where only very slight formation of interface states occurs at the high energy side of the broadened HOMO resonance. As a result of the lack of sulfur hybridization with Pd electron states with energies much different from the HOMO, the HOMO resonance becomes quite localized and strong. As the distance is increased further to 3.5 Å, as in Fig. 1(e), no hybridization of the HOMO into interface states occurs, and the transmission through the HOMO evolves into two closely spaced peaks that are very narrow because of the weakness of the coupling between the molecular thiol groups and the electrodes at this separation; we find the HOMO of the isolated AT4 molecule (that is located primarily on the thiol end groups) to be similarly split.

The trends presented in Fig. 1 can be understood as follows: For large Pd-S separations, the molecule is only weakly coupled to the Pd contacts and so molecular orbitals only weakly transmit. As the separation is decreased, the HOMO couples more strongly to the surface states of the Pd contacts and broad transmitting states begin to form. As the distance is decreased further, the wave function overlaps between the HOMO and Pd surface states with *different* energies become non-negligible, and the HOMO couples to more surface states resulting in stronger hybridization (energetically well-separated quantum states couple and mix together only once their hopping or coupling energies are comparable to their energy spacings). Since the maximum in the Pd DOS is energetically localized and slightly below the Fermi energy and mostly of *d*-electron character[65] [this is true for the surface DOS as well[77]], as the separation is decreased, the HOMO couples to more and more *d*-states near the Fermi

energy, causing the overall upwards shift in energy of the interface state resonances. Near the equilibrium separation these transmitting states are well separated from the HOMO resonance and have evolved into what we have termed interface states. Since the HOMO of AT4 is primarily localized on the sulfurs (only very weakly delocalized on the carbon backbone), as the coupling between the sulfurs and the Pd is increased, the nature of the HOMO changes significantly and the transmission through the HOMO is dramatically affected (reduced).

At this point it is worthwhile to point out a subtle distinction that exists between the coupling between the metal surface states and the sulfur orbitals, which gives rise to interface states [i.e., if the coupling is too weak, no hybridization into interface states occurs] and the coupling between states deep in the lead and the interface states themselves. The latter coupling controls the width and overall shape of the interface state resonances and is strongly dependent on the properties of not only the interface, but of the whole system. Therefore, this coupling is difficult to quantify *a priori*. This is exemplified by the differences in resulting interface state resonances that emerge upon binding the molecule at different surface sites, as discussed in the following section.

Also, as alluded to above, once the equilibrium separation has been reached, the energies of the interface states are strongly correlated with maxima in the bulk and surface metal DOS. For bcc transition metal leads, whose DOS show two distinctly separated maxima, we find interface states resonances to occur near each (see, for example, Ref. 32). For fcc metal leads, interface states such as those displayed in Fig. 1(a) are predicted very near the maximum in the densities of states (bulk and surface DOS are relevant). Their precise energies, however, are dependent on the properties of the interface and of the whole system.

As an aside, it is clear from Fig. 1(b) that if the equilibrium S-Pd separation were 2 Å instead of the 1.74 Å given by our density functional calculations, interface state resonances would still dominate measurable quantities at low bias. Therefore our qualitative predictions are not overly sensitive to the S-Pd separation.

B. Dependence on surface orientation and binding site

Pd can be prepared with either (100) or (111) oriented surfaces and molecules will adsorb on both. We have investigated the effect on the interface states when AT4 molecules adsorb on (111) oriented Pd, with each Pd cluster now built from 55 (in the case of fcc binding site) or 70 (in the case of hcp binding site) Pd atoms. We calculated the transmission when each AT4 molecular sulfur atom is symmetrically bonded over the (111) fcc and hcp hollow sites as well as a bridge site and a bri-fcc site.[81] Again, the thiol-Pd distances in our calculations are based on estimates from density functional calculations[64] and differ for each binding site.

Our calculations reveal interface states to form near the Fermi energy for all binding sites and to be similarly located for all binding sites and surface orientations; subtle differences in the exact energies and differences in the size and shape of the interface state resonances are apparent for the different binding sites. These differences are due to the different geometries, i.e., S-Pd distances, different numbers of S-Pd bonds and different coordination numbers of Pd atoms at the surface, all of which strongly affect the overlaps between sulfur and Pd-*d* electron orbitals. Our results indicate that the hcp binding site gives rise to the strongest interface state resonance, while the bri-fcc site results in the weakest. Both the bridge and bri-fcc site junctions result in the appearance of an interface state resonance closer to the Fermi energy than for the (100) binding site [Fig. 1(a)], while for the hcp site it is only slightly closer. Additionally, the double-peaked interface state transmission feature, as in Fig. 1(a), is present but not as prominent for the fcc binding site while only a single feature is present for the hcp and bridge site. The resonance is more broadened in the case of bri-fcc bonding. Since the transmission resonances near the Fermi energy are associated with interface states, it is not surprising that such differences emerge when switching orientations or binding sites and therefore changing the atomic structure of the interface.

C. Dependence on the length of the molecule

To determine the relationship between interface state transmission and length of the insulating molecule, we have investigated the transmission through molecular junctions where *n*-alkane-dithiolates (with $n=4,6,8$) bridge Pd contacts and found the results to scale with the number of carbon atoms. Both at zero bias, and under finite bias (see Sec. III D below), the calculated transmissions for the three different molecules are quite similar in shape, differing by a scaling factor. We have verified that the transmissions scale as $e^{-\beta n}$ where n is the number of carbons and we find $\beta=1.08$. This can be compared to theoretical results for *n*-alkane-thiolates bridging Ni contacts ($\beta=0.88$),[31] as well as theoretical ($\beta=0.95$),[26] and experimental conducting AFM [$\beta=1.2$ (Ref. 82) and $\beta=0.8$ (Ref. 83)] and STM ($\beta=1.0$) (Ref. 84) results for Au contacts.[85] This scaling of not only the very low bias tunneling background, but also of the resonances associated with the interface states reflects the fact that the interface states allow electrons to resonantly tunnel into and out of the molecule-metal interface, reducing the width of the tunnel barrier. As the length of the molecule increases, so too does the width of the tunnel barrier and the resonances due to interface states scale with the background tunneling transmission.

D. Bias dependence

In the previous sections we have considered the transmission characteristics at zero bias, however, interesting nonlinear current-voltage and behavior of the transmission features due to interface states emerge once the effects of finite bias are explicitly included. The potential profile of a molecular junction arising from the bias voltage applied between the two electrodes is a complex nonequilibrium many-body property, and therefore is difficult to calculate from first principles. However, when treated carefully, appropriate models for the profile can yield accurate results for the current.[86] We

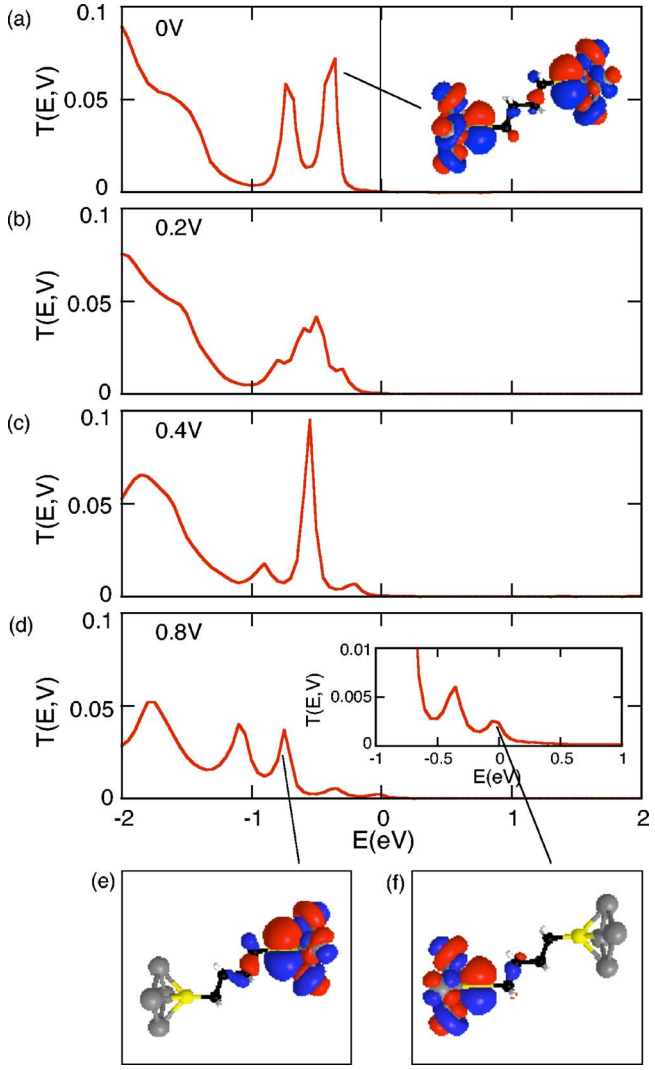

FIG. 2. (Color online) Transmission probabilities $T(E,V)$ as different bias is applied across the molecular junction. (a) Transmission probability vs energy at zero bias. (b) Transmission probability at $0.2V$ bias. (c) $0.4V$. (d) $0.8V$. A closer view of the transmission probability due to interface states near 0 eV is shown in the inset. The applied bias lifts the degeneracy and the interface state in the inset of (a) is replaced with interface states associated with the drain (e) or source (f) electrodes.

adopt this approach here, assuming the majority of the applied bias to drop over the metal-molecule interface;[86–88] we assume that one-third of the applied bias drops at each contact and the remaining one-third drops over the length of the molecule. We apply the bias V symmetrically so that the window of conduction [the limits of integration in Eq.(1)] spans $\pm\frac{eV}{2}$ on either side of the zero bias Fermi energy, $E_F=0$ eV.[89–91] As we show below, our predictions are not sensitive to the details of the assumed potential profile.

The transmission probability as a function of energy for increasing bias for the Pd/AT4/Pd molecular junction is shown in Fig. 2. As shown in Fig. 2(b), compared to the zero bias transmission probability in Fig. 2(a), the applied bias results in an overall decrease of the strength of the resonances associated with the hybridized interface states. The

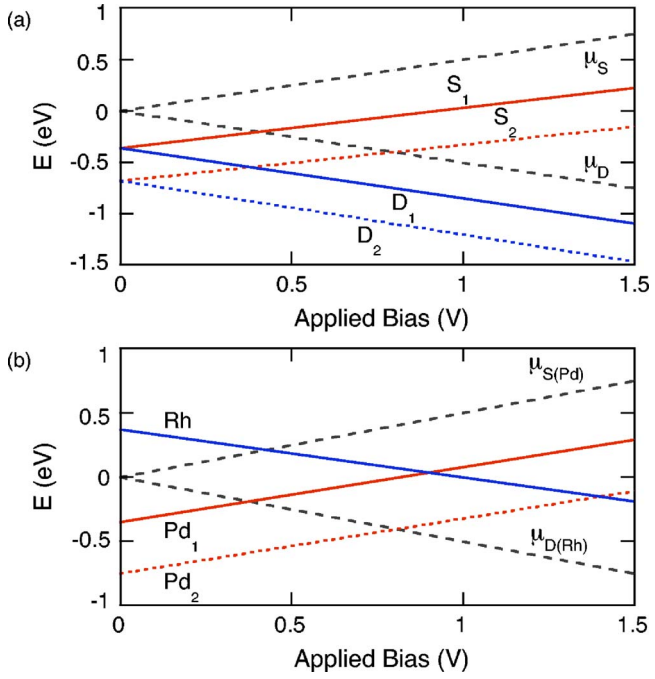

FIG. 3. (Color online) Energies of interface state resonances (solid and dotted lines) and electrode electrochemical potentials (dashed) labeled according to the respective electrode vs bias applied across some metal/molecule/metal junctions. (a) The same Pd/AT4/Pd system as in Figs. 2 and 4(a). S (D) stands for the electron source (drain) electrode, while 1 (2) stands for the high (low) energy interface state. (b) Pd/AT4/Rh junction corresponding to the current plotted in Fig. 4(d).

reason for this is as follows: The wave functions of the interface states responsible for transport at moderate bias are located primarily on the Pd electrodes and are only weakly coupled through the molecule. [The molecular orbital plot in the inset of Fig. 2(a) shows only the portion of the interface states on the molecule and surface layers of the electrodes.] Approximately 90% of the interface state wave functions reside on the Pd electrodes, while the remaining 10% is located primarily on the sulfurs. Therefore the energy levels of the interface states are pinned to the electrodes and follow the electrochemical potentials of the their respective electrodes almost rigidly with applied bias.

This is illustrated in Fig. 3(a) where the energies S_1 and S_2 (D_1 and D_2) of the interface states at the source (drain) Pd electrodes are seen to track the electrochemical potentials μ_S (μ_D) of their respective electrodes. At zero bias, interface states on the source and drain electrode are degenerate, and molecular orbitals form near the Fermi energy with significant wave function weight on *both* source and drain interfaces, as in the inset of Fig. 2(a), resulting in the relatively strong transmission below the Fermi energy in Fig. 2(a). As the interface states on the source and drain move apart with increasing bias, hybridization typically only occurs strongly at one end of the molecule at a given energy and the transmission at those energies is therefore diminished.

This effect is most clearly demonstrated at larger applied bias when the interface state resonances on the source and drain become well separated: Figs. 2(e) and 2(f) show the

effect of 0.8 V applied bias on the interface state displayed in the inset of Fig. 2(a), corresponding to the transmission probability in Fig. 2(d). As the electronic states of the drain electrode are shifted down 0.4 eV in energy, and the source up 0.4 eV in energy, the degeneracy is lifted and the zero bias interface state in Fig. 2(a) is replaced with interface states coupled to either the drain [Fig. 2(e)] or the source [Fig. 2(f)] electrodes. These two separated interface states give rise to the separated resonance peaks [each being the higher energy peak of a double-peaked feature as in Fig. 2(a)] in Fig. 2(d).

This mechanism results in the reduction of the transmission resonance near the Fermi energy as a 0.2 V bias is applied across the molecular junction [Fig. 2(b)]. At 0.4 V applied bias [Fig. 2(c)], the interface states responsible for the lower energy resonance of the double-peaked zero bias interface state transmission feature [near 0.8 eV below the Fermi energy in Fig. 2(a)] shift into resonance with those responsible for the higher energy peak [near 0.4 eV below the Fermi energy in Fig. 2(a)] and the transmission is enhanced at 0.6 eV below the zero bias Fermi energy. As this enhancement of the transmission remains outside of the window of integration in Eq. (1) [interface states D_1 and S_2 cross *outside* of the energy range between μ_S and μ_D at an applied bias of 0.4 V in Fig. 3(a)] it will not directly contribute to the current, but can contribute weakly in an off-resonant fashion. Resonant enhancements and reductions in the transmission, especially when occurring within the current window, can give rise to nonlinear transport phenomena such as NDR, as will be discussed in Sec. III F.

Once the two transmission resonances have passed through one another, the interface states on the source and drain electrode continue to part in a monotonic fashion as in Fig. 2(d). Departure from this trend occurs once the interface states on the drain contact shift into resonance with the broadened HOMO states 1.5–2 eV below the zero bias Fermi energy. As this occurs well outside of the window of integration in Eq. (1) for the low bias results presented here (up to $2V$ in Secs. III F and III G), this will not be discussed further. As the interface states on the source side of the molecule are shifted higher in energy, the double-peaked interface state feature on the source side of the molecule shifts with them, as can be seen in the inset of Fig. 2(d). The magnitude of that transmission feature diminishes as a function of increasing bias, as the interface states are shifted away from the HOMO; surface Pd d states become more energetically separated from the molecular HOMO under bias and the hybridization is weaker (see Sec. III A).

The model potential profile assumed above is expected to be a reasonable approximation to the full self-consistent potential profile. Nevertheless, to assess the dependence of our results on this assumed model profile, we have studied two additional potential profiles: one in which all of the bias drops at the two metal-molecule interfaces, and one in which the applied bias drops linearly between the ends of the two Pd contacts. Nearly identical transmission characteristics to those in Fig. 2 emerge in all bias models. This reflects the fact that the wave functions of the interface states lie primarily within the Pd contacts, and so the energy levels of the interface states are pinned to the electrochemical potentials of the contacts, and move rigidly with applied bias. Therefore measurable quantities such as the current and conductance show no significant differences under the different potential profiles up to $2V$. Thus the details of the model potential profile are not crucial to our predictions at moderate bias.

E. Two-level model of interface states

To better understand the systematics of resonant enhancements in the transmission due to interface molecular orbitals shifting under bias, it is useful to consider a two-level model constructed in the basis of interface states on the source (L) and drain (R) side of the molecule. Any molecular orbital $|\Psi\rangle$ of the extended molecule can be expressed as a linear combination of orbitals on the left $|L\rangle$ and on the right $|R\rangle$ spatial halves of the molecule with some coupling t_{LR} between the two sides (consider, for example, an atomic orbital resolution where every atomic orbital is located either on the left or on the right side of the molecule). When the coupling, t_{LR} between the two sides is very weak,[92,93] much smaller than the spacing between molecular orbital eigenenergies, there is little mixing by the coupling between different orbitals $|L_i\rangle$ and $|R_i\rangle$ and $|L\rangle$ and $|R\rangle$ can be considered eigenvectors of their respective isolated Hamiltonians with eigenvalues ϵ_L and ϵ_R, respectively.[94,95] Since our extended molecule consists of a very large number of orbitals, the energy spacing between molecular orbitals is small and this identification of $|L\rangle$ and $|R\rangle$ is approximate. Nevertheless, we assume for simplicity that the coupling t_{LR} mixes one orbital $|L\rangle$ with one orbital $|R\rangle$, forming two molecular orbitals of the coupled system

$$|\Psi_{1,2}\rangle = a_{1,2}|L\rangle + b_{1,2}|R\rangle, \tag{2}$$

where we may, for instance, make the connection between $|L\rangle$ and the source interface molecular orbital in Fig. 2(f), and $|R\rangle$ and the drain interface molecular orbital in Fig. 2(e).[96] Since the energies of the interface states on the source and drain electrodes are degenerate at zero bias and track rigidly with the source and drain electrochemical potentials under applied bias V we shift the energies of the two-level states accordingly so that $\epsilon_{L,R} = \epsilon \pm \frac{eV}{2}$, where ϵ is the energy location of the interface state resonances at zero bias.

For degenerate energy levels (zero bias) the following two-level Breit-Wigner-like formula[21,74] for the transmission can be derived from the Lippmann-Schwinger scattering equation and the two-level approximation of Eq. (2):

$$T(E) = \frac{4\Gamma_L \Gamma_R t_{LR}^2}{|(E - \epsilon_L + i\Gamma_L)(E - \epsilon_R + i\Gamma_R) - t_{LR}^2|^2}. \tag{3}$$

Here Γ_x is the tunneling rate from the electrodes into the two-level molecule of Eq. (2) and is given by $\Gamma_x = t_x^2 \mathrm{Im}(G_x^{\mathrm{lead}})$, where $x = L, R$ defines the left (source) or right (drain) leads, repsectively, G_x^{lead} is the Green's function of the source and drain leads on the lead sites coupled to the molecule and t_x is the lead-model molecule coupling.[97] Γ_x provides the broadening of the transmission resonances and is associated with the lead's self-energy. For the purposes of

our discussion, we treat it as an empirical parameter used to reproduce the relative sharpness and shape of the interface state transmission resonances.[98] At finite bias $\epsilon_{L,R}=\epsilon\pm\frac{eV}{2}$, the degeneracy is lifted and Eq. (3) is a reasonable approximation and provides an intuitive tool for understanding the nature of the resonances under bias.

It is now straightforward to interpret our transmission results as a function of bias: At zero bias, the transmission resonances associated with the interface states $|L\rangle$ and $|R\rangle$ overlap, both terms in the denominator of Eq. (3) are small at energies near the interface states, and the transmission is enhanced [$|L\rangle$ and $|R\rangle$ are degenerate and $|\Psi\rangle$ is the molecular orbital displayed in the inset of Fig. 2(a)]. As small bias is applied, the resonances begin to part but appreciable overlap between them remains and both of these states continue to contribute coherently to the transmission. As the bias is increased further, the two resonances become well separated, only one term in the denominator of Eq. (3) is small at any energy, and the transmission is no longer enhanced as negligible overlap remains between their off-resonant transmission tails; each interface state now contributes separately to the transmission.

F. Negative differential resistance

In his seminal theoretical paper elucidating NDR in mesoscopic junctions, Lang considered a pair of bulk electrodes in contact through a pair of aluminum atoms.[99] The atoms were weakly bonded to the bulk electrodes and their energy levels did not hybridize strongly with the energy bands of the electrodes; thus the transmitting states near the Fermi energy remained sharp. Lang showed[99] that negative differential resistance is to be expected when sharp transmitting states of such an atomic chain are resonantly shifted past one another under bias. By contrast, for the Pd/AT4/Pd molecular wire considered here, the sharp transmitting states that we predict are due to interface states that form due to strong hybridization between molecular sulfur states and Pd *d*-electron bands; these interface states are located mainly within the contacts (rather than in the wire connecting them as in the system studied by Lang[99]). Nevertheless, as we have shown in Sec. III D and analyzed in Sec. III E, these sharp transmitting states should also move relative to each other under bias, suggesting that such interface states may also give rise to NDR. The present class of systems, being based on metal-thiol chemistry, should be easier to fabricate and much more robust chemically, and thus better suited to potential applications in nanoelectronic devices.

Appreciable NDR is expected when ϵ is close to the Fermi energy so that much of the enhancement and subsequent decrease of the transmission $T(E)$ when interface states are resonantly shifted past one another (see Sec. III E) will enter the window of integration in Eq. (1) when calculating the current as a function of bias. Since $|L\rangle$ and $|R\rangle$ are degenerate at zero bias, and for the Pd/AT4/Pd system $\epsilon\neq E_F$, only a small portion of the resonantly enhanced transmission will enter the window of integration in Eq. (1). Therefore, the magnitude of NDR, determined by the peak-valley ratio of the current, is in this case quite small. This can be seen in Fig. 4(a) where we show the calculated current for the Pd/AT4/Pd molecular junction [depicted in the inset of Fig. 1(a)] as a function of applied bias; this result is obtained from Eq. (1) with $T(E,V)$ as shown in Fig. 2. Although weak, NDR is present near $1V$.

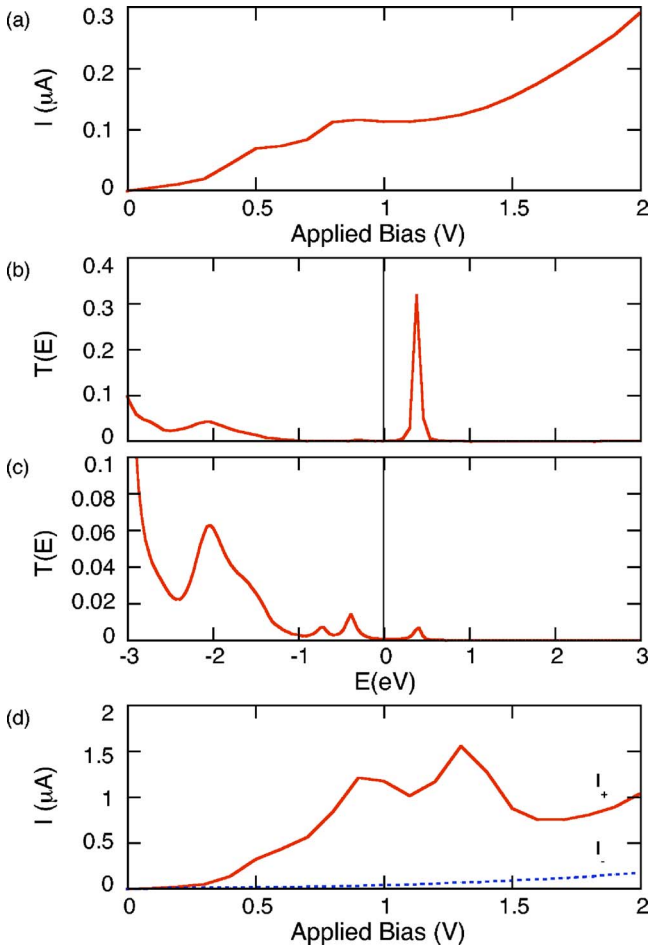

FIG. 4. (Color online) Currents displaying negative differential resistance. (a) $I(V)$ for the Pd/AT4/Pd molecular junction calculated with Eq. (1) and $T(E,V)$ in Fig. 2. (b) Zero bias transmission probability for a Rh/AT4/Rh molecular junction. (c) Transmission probability for a Pd/AT4/Rh molecular junction. (d) $I(V)$ for Pd/AT4/Rh molecular junction. The solid curve is current for forward bias, dashed curve is magnitude of current for reverse bias $|I_-|$. Forward bias induces a net electron flux in the direction from the Pd source electrode to the Rh drain electrode.

For a detailed interpretation of the structure in Fig. 4(a) it is necessary to go beyond a simple two-level model since in reality the interface resonance on *each* Pd electrode is split into a doublet as can be seen in Fig. 2(a). At low bias the current through the Pd/AT4/Pd junction increases with bias in Fig. 4(a) because [as shown in Fig. 3(a)] the transmission resonance due to the high energy interface state on the source electrode (S_1) is approaching the energy window between the source and drain electrochemical potentials ($\mu_{S,D}$) in which [according to Eq. (1)] electron transmission contributes the most effectively to the current. Once the S_1 interface state resonance has fully entered the window, the current begins to plateau until the second transmission feature of the doublet (S_2) approaches and enters the window.

Once S_2 has fully entered the window in Fig. 3(a) the current begins to decrease due to the decaying amplitude of the resonance with increasing bias as it continues to separate in energy from the interface state resonances on the drain (D_1 and D_2); as can be seen in the inset of Fig. 2(d), some small but non-negligible overlap remains close to the edge of the window of integration at $0.8V$. This results in the small NDR near $1V$ in Fig. 4(a).[38] As the bias increases further the current begins to increase again because of the increasing width of the window between μ_S and μ_D and the decreasing importance of the interface state transmission resonances relative to the background transmission due to nonresonant tunneling through the AT4 molecule.

Since enhancements and subsequent decreases in the transmission [the crossing of S_2 and D_1 in Fig. 3(a)] occur outside of the window of integration and contribute only off-resonantly to the current, the full potential NDR via this mechanism will not be realized for degenerate $\epsilon_{L,R}$ (in principle, large NDR could be achieved if $\epsilon_{L,R}=E_F$ but this is not the case here). However we predict stronger NDR to occur in systems for which interface states form on *opposite* sides of the zero bias Fermi energy and thus can be shifted *into* resonance [within the energy window of integration in Eq. (1)] by the application of bias. Energetically separated interface state resonances have been predicted for bcc transition metals, where the DOS contains two well resolved maxima on either side of the Fermi energy [see, for example, spin down Fe in Fig. 1(a) of Ref. 32]. However, in all of the bcc metal-molecule systems we have considered, these interface state resonances are not sharp enough in energy to provide NDR. A mechanism not requiring sharp transmitting states but similarly due to resonant interface state transmission is, however, responsible for our prediction of negative magnetoresistance in Fe-molecular systems;[32] under bias spin up interface states on the source electrode are shifted into resonance with spin down interface states on the drain enhancing the current in the case of antiparallel magnetizations.

Another approach to maximizing NDR via this mechanism is to consider asymmetric fcc contacts where the source electrode has DOS maxima below the zero bias Fermi energy, as for Pd, while the drain electrode has DOS maxima above the Fermi energy (both surface and bulk DOS are relevant). Substituting a (100) rhodium electrode for the Pd drain electrode of the molecular junction shown in the inset of Fig. 1(a) satisfies this criterion:[65] The zero bias transmission probability is shown in Fig. 4(b) for AT4 bridging symmetric (100) Rh contacts. Here the contacts are again constructed from 54 Rh atoms arranged in a bulk Rh fcc geometry and the equilibrium S-Rh separation is predicted to be 1.82 Å;[64] our qualitative predictions are not sensitive to this separation.[100] Near 2 eV below the Fermi energy, there is weak transmission due to the broadened HOMO, but more importantly, a strong, sharp interface resonance resonance appears just above the Fermi energy. Thus the combined Pd/AT4/Rh system possesses a doubly peaked interface state on the Pd source side below the zero bias Fermi energy that will be shifted into, and subsequently out of, resonance with the interface state on the Rh drain side which is above the Fermi energy as displayed in Fig. 4(c). The interface state resonances are weaker in Fig. 4(c) than in either Fig. 2(a) or 4(b) as interface states form only on one side of the molecular junction at a particular energy.

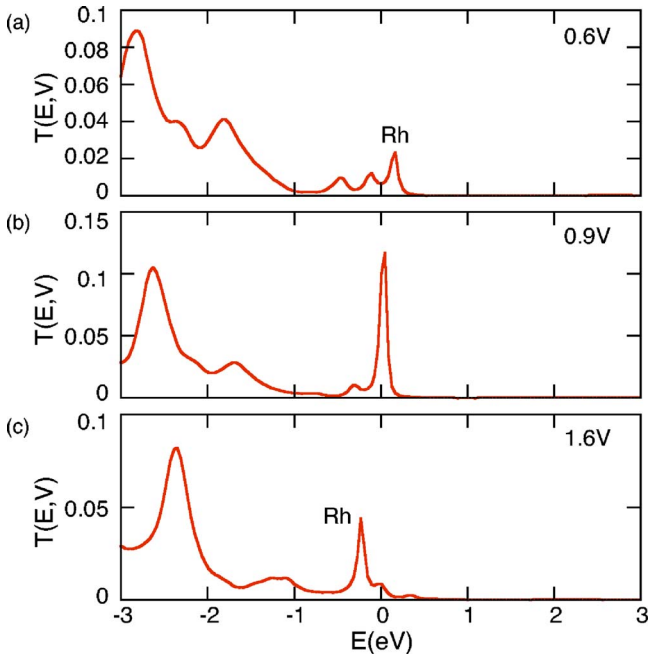

FIG. 5. (Color online) Transmission probabilities $T(E,V)$ as different bias is applied across the Pd/AT4/Rh molecular junction. (a) Transmission probability vs energy at $0.6V$. (b) $0.9V$ bias. (c) $1.6V$.

The predicted currents for the Pd/AT4/Rh molecular junction are shown in Fig. 4(d). Since the work functions of Pd and Rh are different, once AT4 has bridged the leads, a current will flow between to two contacts until an equilibrium Fermi energy has been established, creating an electric field in the vicinity of the molecule. This electric field is treated in an similar way to that created by application of bias, where the molecular energy levels are shifted under the assumed potential profile, as discussed in Sec. III D.[101,102] Pronounced NDR is apparent in the forward bias direction [solid curve in Fig. 4(d)] near $1.1V$ and $1.6V$. (Forward bias is defined as the bias that causes electrons to flow from the source Pd electrode to the drain Rh electrode.) The two occurrences of NDR are related to the double-peaked feature in the Pd interface state transmission in Fig. 4(c): The sharp Rh interface state resonance above the Fermi energy in Fig. 4(c) scans both Pd interface transmission resonances, as depicted in Fig. 3(b) by the crossing of the Rh interface state resonance with the high (Pd_1) and low (Pd_2) energy Pd interface states resonances near $0.9V$ and $1.4V$, respectively. Thus there are two enhancements and subsequent decreases in the transmission within the window of integration between μ_S and μ_D in Fig. 3(b), corresponding to the two peaks and valleys in the current in Fig. 4(d).

The effect of applied bias on the interface states in Fig. 4(c) is clearly demonstrated in Fig. 5 where we plot the transmission probability for increasing bias voltage applied to the Pd/AT4/Rh molecular junction. In Fig. 5(a) for $0.6V$ applied bias, the separation between the energies of the interface states on the Pd and Rh (labeled Rh) contacts has decreased relative to that in Fig. 4(c). At an applied bias of

0.9V [Fig. 5(b)], the interface state Pd_1 shifts into resonance with the Rh state (the resonantly transmitting state has strong contributions at both metal-molecule interfaces) and the transmission is greatly enhanced (note also the change in y-axis scale), corresponding to the maximal current in Fig. 4(d). At 1.6V, the Rh interface state has shifted past both Pd states and the transmission has weakened, corresponding to the NDR in Fig. 4(d).

The predicted significant NDR for Pd/AT4/Rh suggests potential avenues for controlling negative differential resistance in molecular junctions: By choosing metal contacts with appropriate electronic structure, it is possible to manipulate interface states that dominate the transmission at moderate bias. Though our qualitative predictions are robust, quantitative current-voltage characteristics, and values of NDR, are dependent on the interface properties of the molecular junction: Since the geometry and interface properties in general depend on how samples are fabricated,[22] our results suggest that improved control over sample preparation may offer further control over NDR transport phenomena. Also, since transmission enhancements due to interface states on the source electrode shifting into resonance with interface states on the drain do not involve any structural rearrangement of the molecule or contacts, this mechanism for NDR is not expected to be accompanied by hysteresis. Since hysteresis has been found experimentally in many metal/molecule/metal devices exhibiting NDR to date, *lack* of hysteresis accompanying the NDR in a molecular device in which d-electron interface states are expected should be an important experimental characteristic of the NDR mechanism that we have proposed here.

It is clear that because this NDR mechanism requires the relative shifting of interface states on the source (Pd) upwards in energy and into resonance with interface states on the drain (Rh), NDR will only occur in one direction of applied bias. In fact, in the reverse direction of bias, no significant transmission features enter the window of integration and the current is weak as displayed by the dashed curve in Fig. 4(d) (we plot $|I_-|$ vs $|V|$ in the same quadrant as positive bias for easy comparison). Therefore, we predict the Pd/AT4/Rh molecular junction to also act as a rectifier, yielding appreciable rectification.

G. Rectification

To explore our prediction of molecular rectification further, we now investigate the possibility of rectification when molecules form a bridge between Pd and Au contacts. Again we consider here (100) surface orientations; we find very similar results for other surface orientations and binding sites. Here we take the Au-S separation to be 2 Å as predicted with density functional calculations,[64] where the sulfur adsorbs above fourfold Au hollow sites.

The transmission and currents for both directions of bias for the Pd/AT4/Au molecular junction are shown in Fig. 6. The double-peaked interface state transmission resonances below the Fermi energy in Fig. 6(a) are weaker than those in Fig. 2(a) as interface states form there only on one (the Pd) contact for the Pd/AT4/Au system; as alluded to earlier in-

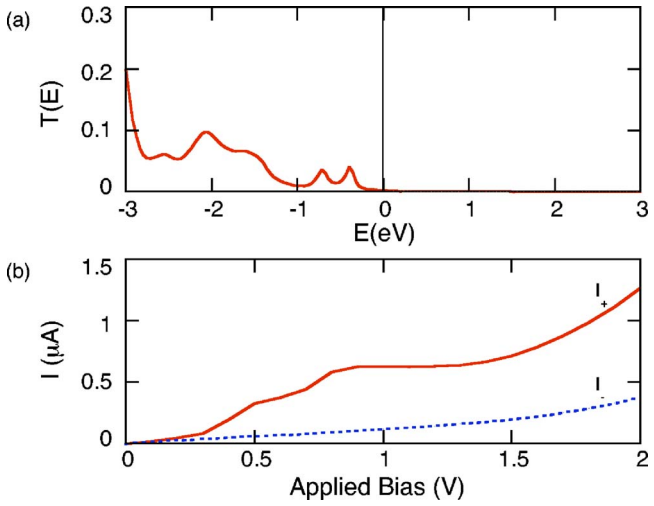

FIG. 6. (Color online) Currents displaying rectification. (a) Transmission probability at zero bias for a Pd/AT4/Au molecular junction. (b) $I(V)$ for Pd/AT4/Au molecular junction. Solid curve is current for forward bias, dashed curve for reverse bias. Forward bias induces a net electron flux in the direction from the Pd source electrode to the Au drain electrode.

terface states do not form near the Fermi energy on the Au contact. The solid curve of Fig. 6(b) is the current for the forward bias direction I_+; the dashed curve is the current for the reverse direction $|I_-|$. As can be seen I_+ saturates near 1V, once both Pd interface transmission features in Fig. 6(a) have completely entered the window of integration. The shape of the current profile is quite similar to that predicted for Pd/AT4/Pd [Fig. 4(a)] because the latter current is dominated by resonant transmission from interface state resonances on the source once they enter the window of integration [see Fig. 2(d), inset and Fig. 3(a)], which are also present for Pd/AT4/Au [Fig. 6(a)], and is only weakly modified by off resonant transmission tails of interface states on the Pd/AT4/Pd drain electrode, that are not present for Pd/AT4/Au. However, there is no appreciable NDR for Pd/AT4/Au.

In the reverse bias direction [dashed curve in Fig. 6(b)], no appreciable transmission features enter the window of integration; the interface state resonances on the source shift with the electrochemical potentials of the Pd contact and remain outside of the current window [as in Fig. 3(a) for $D_{1,2}$], while no significant transmission features are present near the Fermi energy on the Au contact. Therefore, an appreciable rectification ratio ($I_+/|I_-|$) is predicted, reaching a value of about 6 near the 1V saturation bias.

Since the rectification in this system emerges from interface states forming on the S-Pd contact and the lack of interface states on the S-Au contact, increasing the asymmetry by switching to a molecule with a single thiol does not drastically increase the rectification, provided the thiol bonds to the Pd contact.[103] In fact we predict quite similar current-voltage characteristics for Pd/butyl-thiolate/Au to those in Fig. 6(b) up to a scaled decrease in the magnitudes of both forward and reverse currents due to the lack of direct bonding at the Au interface. Similar rectification is predicted for symmetric Pd leads bridged with an asymmetric molecule such as butyl-thiolate where significant interface states also form only on one side of the junction.

Therefore interface states can provide rectification in such asymmetric systems: Resonances associated with interface states close to the zero bias Fermi energy shift rigidly (pinned to one contact) with bias but occur only on one side of molecule, either because only one contact is bonded to the molecule or because no *d* states are present near the Fermi energy for one of the electrodes. Therefore, interface state resonances will enter the current window in Eq. (1) only in one direction of applied bias. Since we find transport via interface state resonances to scale with the length of the alkane chain, our analysis should be generally applicable to thiolated molecules that possess at least one thiol-end when interface state resonances within the molecular HOMO-LUMO gap are the dominant transmission feature near the Fermi energy of the metal-molecule junction.

IV. CONCLUSION

We have presented calculations indicating that interface states in molecular junctions should play a nontrivial role in transport when *d*-electron orbitals of the metal electrodes make a significant contribution to the density of states of the metal near the Fermi energy. As an example, we considered in detail a molecular junction where butyl-dithiolate bridges Pd contacts and determined that electron transmission through the junction at moderate bias is dominated by interface states resulting from hybridization between the thiolated ends of the molecule and the Pd *d* orbitals. We predicted resonant enhancements and reductions in the transmission due to interface states to occur when a bias is applied across the junction and showed that this should result in nonlinear transport phenomena including negative differential resistance and rectification. Potential avenues for tailoring these non-linear transport phenomena were also considered by replacing one Pd electrode with other transition metals: Integration of an Au electrode was predicted to produce appreciable rectification, while the inclusion of an Rh electrode was predicted to yield both strongly enhanced NDR and rectification. The interface state resonances were found to be only weakly dependent on the details of the model potential profile between the metal contacts and the transmission mediated by those interface state resonances was found to scale with the length of the insulating molecule, suggesting our results may be applicable to a variety of thiolated molecules. Factors such as the surface orientation of the metal interface, the adsorption site of the molecule and the separation between the thiolated molecule and the Pd surface were found to strongly affect the characteristics of the interface states. Therefore, the specific atomic parameters of the interface are expected to play a crucial role in the emergence of interface states and their resonant enhancements leading to nonlinear transport phenomena. Further control and characterization of interface parameters should allow for the control of resonances due to interface states, and may provide a useful tool for engineering molecular electronic junctions for specific applications.

ACKNOWLEDGMENTS

We are grateful to Ross Hill and Brad Johnson for stimulating discussions. This work was supported by NSERC and the Canadian Institute for Advanced Research.

[1] For reviews see J. R. Heath and M. A. Ratner, Phys. Today **56** (5), 43 (2003); A. Salomon, D. Cahen, S. Lindsay, J. Tomfohr, V. B. Engelkes, and C. D. Frisbie, Adv. Mater. (Weinheim, Ger.) **15**, 1881 (2003); D. M. Adams, L. Brus, C. E. D. Chidsey, S. Creager, C. Creutz, C. R. Kagan, P. V. Kamat, M. Lieberman, S. Lindsay, R. A. Marcus, R. M. Mertzger, M. E. Michel-Beyerle, J. R. Miller, M. D. Newton, D. R. Rolison, O. Sankey, K. S. Schanze, J. Yardley, and X. Zhu, J. Phys. Chem. B **107**, 6668 (2003); S. M. Lindsay, Electrochem. Soc. Interface **13**, 26 (2004); M. C. Hersam and R. G. Reifenberger, MRS Bull. **29**, 285 (2004).

[2] E. G. Emberly and G. Kirczenow, Phys. Rev. B **58**, 10911 (1998).

[3] S. N. Yaliraki, M. Kemp, and M. A. Ratner, J. Am. Chem. Soc. **121**, 3428 (1999).

[4] J. M. Seminario, A. G. Zacarias, and J. M. Tour, J. Am. Chem. Soc. **121**, 411 (1999).

[5] M. Di Ventra, S. T. Pantelides, and N. D. Lang, Phys. Rev. Lett. **84**, 979 (2000); M. Di Ventra and N. D. Lang, Phys. Rev. B **65**, 045402 (2002); M. Di Ventra, N. D. Lang, and S. T. Pantelides, Chem. Phys. **281**, 189 (2002).

[6] J. M. Seminario, C. E. De La Cruz, and P. A. Derosa, J. Am. Chem. Soc. **123**, 5616 (2001).

[7] P. E. Kornilovitch and A. M. Bratkovsky, Phys. Rev. B **64**, 195413 (2001); A. M. Bratkovsky and P. E. Kornilovitch, *ibid.* **67**, 115307 (2003).

[8] A. W. Ghosh and S. Datta, J. Comput. Electron. **1**, 515 (2002).

[9] J. Reichert, R. Ochs, D. Beckmann, H. B. Weber, M. Mayor, and H. v. Löhneysen, Phys. Rev. Lett. **88**, 176804 (2002).

[10] J. G. Kushmerick, D. B. Holt, J. C. Yang, J. Naciri, M. H. Moore, and R. Shashidhar, Phys. Rev. Lett. **89**, 086802 (2002).

[11] J. Taylor, M. Brandbyge, and K. Stokbro, Phys. Rev. Lett. **89**, 138301 (2002).

[12] G. K. Ramachandran, T. J. Hopson, A. M. Rawlett, L. A. Nagahara, A. Primak, and S. M. Lindsay, Science **300**, 1413 (2003).

[13] Y. Xue and M. A. Ratner, Phys. Rev. B **68**, 115407 (2003); **69**, 085403 (2004).

[14] X. Xiao, B. Xu, and N. J. Tao, Nano Lett. **4**, 267 (2004).

[15] D. R. Stewart, D. A. A. Ohlberg, Y. Chen, R. S. Williams, J. O. Jeppesen, K. A. Nielsen, and J. F. Stoddart, Nano Lett. **4**, 133 (2004).

[16] G. C. Liang, A. W. Ghosh, M. Paulsson, and S. Datta, Phys. Rev. B **69**, 115302 (2004).

[17] S. I. Khondaker, Z. Yao, L. Cheng, J. C. Henderson, Y. Yao, and J. M. Tour, Appl. Phys. Lett. **85**, 645 (2004).

[18] N. B. Zhitenev, A. Erbe, and Z. Bao, Phys. Rev. Lett. **92**, 186805 (2004).

[19] W. T. Geng, J. Nara, and T. Ohno, Appl. Phys. Lett. **85**, 5992

(2004).
[20] S.-H. Ke, H. U. Baranger, and W. Yang, J. Chem. Phys. **122**, 074704 (2005).
[21] B. Larade and A. M. Bratkovsky, Phys. Rev. B **72**, 035440 (2005).
[22] Y. Hu, Y. Zhu, H. Gao, and H. Guo, Phys. Rev. Lett. **95**, 156803 (2005).
[23] S. Datta, W. Tian, S. Hong, R. Reifenberger, J. I. Henderson, and C. P. Kubiak, Phys. Rev. Lett. **79**, 2530 (1997).
[24] E. G. Emberly and G. Kirczenow, Phys. Rev. Lett. **87**, 269701 (2001); Phys. Rev. B **64**, 235412 (2001).
[25] P. A. Derosa and J. M. Seminario, J. Phys. Chem. B **105**, 471 (2001).
[26] C. Kaun and H. Guo, Nano Lett. **3**, 1521 (2003).
[27] Molecular junctions based on Ag, Cu, Al have also been considered with results comparable to those for Au Refs. 3 and 6.
[28] E. G. Emberly and G. Kirczenow, Chem. Phys. **281**, 311 (2002).
[29] R. Pati, L. Senapati, P. M. Ajayan, and S. K. Nayak, Phys. Rev. B **68**, 100407(R) (2003).
[30] W. I. Babiaczyk and B. R. Bulka, J. Phys.: Condens. Matter **16**, 4001 (2004).
[31] A. R. Rocha, V. M. García-Suárez, S. W. Bailey, C. J. Lambert, J. Ferrer, and S. Sanvito, Nat. Mater. **4**, 335 (2005).
[32] H. Dalgleish and G. Kirczenow, Phys. Rev. B **72**, 184407 (2005).
[33] W. T. Geng, J. Nara, and T. Ohno, Thin Thin Solid Films **464-465**, 379 (2004).
[34] W. T. Geng, H. Kondo, J. Nara, and T. Ohno, Phys. Rev. B **72**, 125421 (2005).
[35] R. H. M. Smit, Y. Noat, C. Untiedt, N. D. Lang, M. C. van Hemert, and J. M. van Ruitenbeek, Nature (London) **419**, 926 (2002).
[36] V. M. Garcia-Suarez, A. R. Rocha, S. W. Bailey, C. J. Lambert, S. Sanvito, and J. Ferrer, Phys. Rev. B **72**, 045437 (2005).
[37] X. J. Wu, Q. X. Li, and J. L. Yang, Phys. Rev. B **72**, 115438 (2005).
[38] Our findings for Pt contacts are qualitatively similar to those for Pd; see H. Dalgleish and G. Kirczenow, Nano Lett. **6**, 1274 (2006).
[39] Analogous locking of interface state energies to the electrochemical potentials of Fe contacts under bias was introduced in Ref. 32.
[40] A number of possible explanations of NDR in molecular junctions have been proposed including: current-induced charging or conformational changes in the molecules (Refs. 41–48), metal filaments (Ref. 49), or impurities (Refs. 21 and 50) within the molecular layer, bond fluctuation (Ref. 17), vibronic mediation (Refs. 51 and 52), and polaron formation (Ref. 53).
[41] J. Chen, M. A. Reed, A. M. Rawlett, and J. M. Tour, Science **286**, 1550 (1999); J. Chen, W. Wang, M. A. Reed, A. M. Rawlett, D. W. Price, and J. M. Tour, Appl. Phys. Lett. **77**, 1224 (2000).
[42] A. M. Rawlett, T. J. Hopson, L. A. Nagahara, R. K. Tsui, G. K. Ramachandran, and S. M. Lindsay, Appl. Phys. Lett. **81**, 3043 (2002).
[43] N. Gergel, N. Majumdar, K. Keyvanfar, N. Swami, L. R. Harriott, J. C. Bean, G. Pattanaik, G. Zangari, Y. Yao, and J. M. Tour, J. Vac. Sci. Technol. A **23**, 880 (2005).
[44] J. M. Seminario, A. G. Zacarias, and J. M. Tour, J. Am. Chem. Soc. **120**, 3970 (1998); **122**, 3015 (2000); J. M. Seminario, A. G. Zacarias, and P. D. Derosa, J. Phys. Chem. A **105**, 791 (2001).
[45] E. G. Emberly and G. Kirczenow, Phys. Rev. B **64**, 125318 (2001).
[46] M. Di Ventra, S. T. Pantelides, and N. D. Lang, Phys. Rev. Lett. **88**, 046801 (2002).
[47] J. Cornil, Y. Karzazi, and J. L. Brédas, J. Am. Chem. Soc. **124**, 3516 (2002).
[48] J. Taylor, M. Brandbyge, and K. Stokbro, Phys. Rev. B **68**, 121101(R) (2003).
[49] C. N. Lau, D. R. Stewart, R. S. Williams, and M. Bockrath, Nano Lett. **4**, 569 (2004).
[50] L. H. Yu and D. Natelson, Nanotechnology **15**, S517 (2004).
[51] J. Gaudioso, L. J. Lauhon, and W. Ho, Phys. Rev. Lett. **85**, 1918 (2000).
[52] S. Lakshmi and S. K. Pati, J. Chem. Phys. **121**, 11998 (2004).
[53] M. Galperin, M. A. Ratner, and A. Nitzan, Nano Lett. **5**, 125 (2005).
[54] T. Rakshit, G.-C. Liang, A. W. Ghosh, and S. Datta, Nano Lett. **4**, 1803 (2004); T. Rakshit, G.-C. Liang, A. W. Ghosh, M. C. Hersam, and S. Datta, Phys. Rev. B **72**, 125305 (2005).
[55] A. Aviram and M. A. Ratner, Chem. Phys. Lett. **29**, 277 (1974).
[56] V. Mujica, M. Kemp, A. Roitberg, and M. Ratner, J. Chem. Phys. **104**, 7296 (1996); V. Mujica, M. A. Ratner, and A. Nitzan, Chem. Phys. **281**, 147 (2002).
[57] A. Dhirani, P.-H. Lin, P. Guyot-Sionnest, R. W. Zehner, and L. R. Sita, J. Chem. Phys. **106**, 5249 (1997).
[58] C. Zhou, M. R. Deshphande, M. A. Reed, L. Jones II, and J. M. Tour, Appl. Phys. Lett. **71**, 611 (1997).
[59] C. Krzeminski, C. Delerue, G. Allan, D. Vuillaume, and R. M. Metzger, Phys. Rev. B **64**, 085405 (2001).
[60] P. E. Kornilovitch, A. M. Bratkovsky, and R. S. Williams, Phys. Rev. B **66**, 165436 (2002); B. Larade and A. M. Bratkovsky, *ibid.* **68**, 235305 (2003); S.-C. Chang, Z. Li, C. N. Lau, B. Larade, and R. S. Williams, Appl. Phys. Lett. **83**, 3198 (2003).
[61] F. Zahid, A. W. Ghosh, M. Paulsson, E. Polizzi, and S. Datta, Phys. Rev. B **70**, 245317 (2004).
[62] R. M. Metzger, Macromol. Symp. **212**, 63 (2004).
[63] G. Ho, J. R. Heath, M. Kondratenko, D. F. Perepichka, K. Arseneault, M. Pézolet, and M. R. Bryce, Chem.-Eur. J. **11**, 2914 (2005).
[64] The GAUSSIAN 03 package (Rev. B.05) was used with the B3PW91 density functional and the Lanl2DZ basis set.
[65] D. A. Papaconstantopoulos, *Handbook of the Band Structure of Elemental Solids* (Plenum Press, New York, 1986).
[66] Some previous studies have indicated that small Pd nanoclusters possess weak ferromagnetism, but that magnetism is limited to very small nanoclusters and even then is controversial (Ref. 67). As our Pd clusters are of appreciable size (54 atoms) and employed to model real macroscopic leads [our previous studies have indicated that 54 atom clusters are large enough to model bulk leads (Ref. 71)], ferromagnetism is not relevant here.
[67] T. Futschek, M. Marsman, and J. Hafner, J. Phys.: Condens. Matter **17**, 5927 (2005).
[68] Y. Xie and J. A. Blackman, Phys. Rev. B **64**, 195115 (2001).
[69] J. Rogan, G. García, J. A. Valdivia, W. Orellana, A. H. Romero, R. Ramírez, and M. Kiwi, Phys. Rev. B **72**, 115421 (2005).
[70] I. Efremenko and M. Sheintuch, Surf. Sci. **414**, 148 (1998).
[71] H. Dalgleish and G. Kirczenow, Phys. Rev. B **72**, 155429 (2005).
[72] O. Šipr, M. Košuth, and H. Ebert, Phys. Rev. B **70**, 174423 (2004).
[73] J. Velev and W. H. Butler, Phys. Rev. B **69**, 094425 (2004).

[74] J. C. Cuevas, J. Heurich, F. Pauly, W. Wenzel, and G. Schön, Nanotechnology **14**, R29 (2003).
[75] S. P. McGlynn, L. G. Vanquickenborne, M. Kinoshita, and D. G. Carrol, *Introduction to Applied Quantum Chemistry* (Holt, Rinehart, Winston, New York, 1972), Chaps. 2–4.
[76] For a review see S. Datta, *Electronic Transport in Mesoscopic Systems* (Cambridge University Press, Cambridge, 1995).
[77] J. G. Gay, J. R. Smith, F. J. Arlinghaus, and T. W. Capehart, Phys. Rev. B **23**, 1559 (1981).
[78] The sensitivity of the interface states to charging effects was also investigated by shifting the atomic orbitals of the molecule in energy relative to those of the metal contacts to simulate qualitatively possible effects of changes in the potential distribution associated with charging. The HOMO energy was found to be sensitive to such shifts while the interface state energies were not, being pinned to features in the d-band density of states of the contacts, although the strength of the interface state resonances was influenced by such shifts. Thus charging effects may influence our quantitative results but our qualitative predictions are expected to be robust.
[79] H. Dalgleish and G. Kirczenow (unpublished). Also see Fig. 6(a).
[80] A detailed account of the influence of bulk and surface densities of states on transport has been provided for a nanoscale junction of Fe leads (for which *d*-electron states are equally important) in Ref. 71.
[81] Y. Yourdshahyan and A. M. Rappe, J. Chem. Phys. **117**, 825 (2002).
[82] D. J. Wold and C. D. Frisbie, J. Am. Chem. Soc. **123**, 5549 (2001).
[83] X. D. Cui, X. Zarate, J. Tomfohr, O. F. Sankey, A. Primak, A. L. Moore, T. A. Moore, D. Gust, G. Harris, and S. M. Lindsay, Nanotechnology **13**, 5 (2002).
[84] B. Xu and N. Tao, Science **301**, 1221 (2003).
[85] See also W. Wang, T. Lee, and M. A. Reed, Phys. Rev. B **68**, 035416 (2003).
[86] S.-H. Ke, H. U. Baranger, and W. Yang, Phys. Rev. B **70**, 085410 (2004).
[87] V. Mulica, A. E. Roitberg, and M. Ratner, J. Chem. Phys. **112**, 6834 (2000).
[88] P. S. Damle, A. W. Ghosh, and S. Datta, Phys. Rev. B **64**, 201403 (2001).
[89] The calculations presented here were carried out for zero temperature.
[90] The bias is applied explicitly as follows: All Pd atoms (and ideal leads) to the source side of the molecule are assumed to be at a potential $\phi=-\frac{V}{2}$, while Pd atoms and leads to the drain side are at $+\frac{V}{2}$. The atoms making up the molecule then are subject to a linear potential following the assumed potential profile, where $\phi=\frac{1}{3}\frac{Vx}{2}$, where x is the position of the molecule's constituent atoms in the direction of electronic flux, relative to the center of the molecule.
[91] This spatially nonuniform potential profile is incorporated into our tight binding Hamiltonian as discussed in Ref. 28, Appendix A and in Ref. 71, Sec. IV. A.
[92] As the interface states are localized on the metal-molecule interface (as opposed to delocalized over the carbon backbone) the magnitude of t_{LR} should reflect the effective coupling through the entire carbon backbone (Ref. 93), and not just the coupling between the left and right sides due to a single C-C bond; t_{LR} should be small, representative of the coupling between the interface states on the source and drain sides of the molecular junction.
[93] J. W. Evenson and M. Karplus, J. Chem. Phys. **96**, 5272 (1992).
[94] A similar two-level analysis has been performed in Ref. 95.
[95] P. Delaney, M. Nolan and J. C. Greer, J. Chem. Phys. **122**, 044710 (2205).
[96] At any particular energy E one of the two split levels on each electrode is closer to E_F than the other, and therefore to a first approximation only the closer of the split levels is included reducing the multistate problem to a two level one.
[97] Equation (3) is exact if the molecular levels are "renormalized." That is if the term $t_x^2\mathrm{Re}(G_x^{\mathrm{lead}})$ is added to $\epsilon_{L,R}$ (Ref. 74)
[98] In the physical model, Γ represents the coupling between a state deep within the contacts and the interface states and depends on V, E, and details of the entire system Hamiltonian and is difficult to quantify *a priori*.
[99] N. D. Lang, Phys. Rev. B **55**, 9364 (1997).
[100] If a Rh-S separation of 2 Å is assumed, the transmission (and resulting current calculations) are not significantly affected. In fact, for 2 Å separation, the interface state resonance occurs closer to the Fermi energy causing and earlier onset of NDR. It is only slightly diminished in magnitude.
[101] We have also carried out calculations for other choices of the model potential profile arising from the difference in work function between Rh and Pd and found almost identical results. The reason for this insensitivity to the details of the potential profile is that the interface states that mediate transport in this system are located mainly within the metal contacts while the insulating AT4 molecule behaves qualitatively as a simple potential barrier; thus neither is sensitive to the details of how the electrostatic potential drops between the metal contacts.
[102] The current-voltage calculation has also been performed with qualitatively similar results assuming another potential profile (in addition to those in Sec. III D) that may develop as a result of a bias voltage applied to the junction. Under this alternate profile, the applied bias was assumed to drop linearly across the region containing the molecule and the first metal layer of each contact. Since the effect of the applied bias on the interface states which are located primarily on the surface layer of each contact is reduced for this profile, the onset of NDR was simply shifted slightly (by 0.1–0.2 V) to higher bias.
[103] No significant rectification is expected if thiols bond only to the Au contact. In this case, interface states are not expected to be significant.